

# Evaluation of High Level Waste Sludge Processing Behavior

December 2023

Amy M Westesen  
Kyleigh J Murray  
Austin A Bachman  
Carolyn A Burns  
Trevor S Scott  
Jessica Rigby  
Reid A Peterson

## DISCLAIMER

This report was prepared as an account of work sponsored by an agency of the United States Government. Neither the United States Government nor any agency thereof, nor Battelle Memorial Institute, nor any of their employees, makes **any warranty, express or implied, or assumes any legal liability or responsibility for the accuracy, completeness, or usefulness of any information, apparatus, product, or process disclosed, or represents that its use would not infringe privately owned rights.** Reference herein to any specific commercial product, process, or service by trade name, trademark, manufacturer, or otherwise does not necessarily constitute or imply its endorsement, recommendation, or favoring by the United States Government or any agency thereof, or Battelle Memorial Institute. The views and opinions of authors expressed herein do not necessarily state or reflect those of the United States Government or any agency thereof.

PACIFIC NORTHWEST NATIONAL LABORATORY  
*operated by*  
BATTELLE  
*for the*  
UNITED STATES DEPARTMENT OF ENERGY  
*under Contract DE-AC05-76RL01830*

Printed in the United States of America

Available to DOE and DOE contractors from  
the Office of Scientific and Technical Information,  
P.O. Box 62, Oak Ridge, TN 37831-0062

[www.osti.gov](http://www.osti.gov)

ph: (865) 576-8401

fox: (865) 576-5728

email: [reports@osti.gov](mailto:reports@osti.gov)

Available to the public from the National Technical Information Service  
5301 Shawnee Rd., Alexandria, VA 22312

ph: (800) 553-NTIS (6847)

or (703) 605-6000

email: [info@ntis.gov](mailto:info@ntis.gov)

Online ordering: <http://www.ntis.gov>

# Evaluation of High Level Waste Sludge Processing Behavior

December 2023

Amy M Westesen  
Kyleigh J Murray  
Austin A Bachman  
Carolyn A Burns  
Trevor S Scott  
Jessica Rigby  
Reid A Peterson

Prepared for  
the U.S. Department of Energy  
under Contract DE-AC05-76RL01830

Pacific Northwest National Laboratory  
Richland, Washington 99354

## Summary

This report summarizes the work performed under FY23 LDRD “Evaluation of HLW Sludge Processing Behavior”. The U.S. Department of Energy’s (DOE) Hanford Site has 177 underground storage tanks that contain wastes from past nuclear fuel reprocessing and waste-management operations. Over 20% of this waste is in the form of an insoluble sludge that will require slurry modification before its transfer to the Waste Treatment and Immobilization Plant (WTP). Specific WTP acceptance criteria for waste feed delivery describe the physical and chemical characteristics of the waste that must be met before the waste is transferred to the WTP. One challenging requirement relates to the undissolved solids (UDS) composition in a waste feed because the waste contains solid particles that settle, and their concentration and relative proportion can change during the transfer of the waste in individual batches. A key uncertainty is the ability to transfer and mix wastes with large variations in UDS concentrations and resulting settling rates. To address this uncertainty, a number of small scale mixing and settling tests have been conducted to determine the mobilization performance of variable chemistry simulants.

Comparison of the size and density of the particulate for each simulant to that of southeast area Hanford sludge was made using metrics for particle mobilization, suspension, settling, and pipeline transfer where dependence on particle size and density may be different, including:

1. Settling velocity
2. Critical shear stress for erosion
3. Just-suspended impeller speed
4. Pipeline critical transport velocity

Existing high-level waste sludge data has shown the effect that increasing Al concentration has on resulting settled solids. This differential settling of particles in the sludge has the possibility of resulting in solids segregation during feed preparation and uneven particle distribution during pipeline transportation or mixer jet pump operations. Understanding the predictive capabilities of HLW solids settling and transport as well as potential remedies for addressing disparate sludge behaviors can help provide technical guidance during HLW flowsheet planning.

## Acknowledgments

This research was supported by the **EED Seed Investment**, under the Laboratory Directed Research and Development (LDRD) Program at Pacific Northwest National Laboratory (PNNL). PNNL is a multi-program national laboratory operated for the U.S. Department of Energy (DOE) by Battelle Memorial Institute under Contract No. DE-AC05-76RL01830. The authors thank Emily Campbell for conducting the technical review of this report and Matt Wilburn for his technical editing contribution on this report.

## Contents

Abstract.....	<b>Error! Bookmark not defined.</b>
Summary .....	<b>Error! Bookmark not defined.</b>
Acknowledgments.....	iii
1.0 Introduction .....	6
2.0 Background and Metrics.....	7
3.0 Experimental Methods.....	8
3.1 Characteristics of SE Area Sludge.....	8
3.2 Settling Velocity .....	9
3.3 Shear Strength Measurements .....	10
3.4 Mixing Evaluation.....	10
4.0 Results .....	11
4.1 Impact of Al Content on Settle Solids.....	11
4.2 Rheology of Samples.....	14
4.3 Solid Suspension Mixing Experiments .....	15
5.0 Conclusions.....	18
6.0 References.....	20

## Figures

Figure 1 Sources of Sludge in the SE Quadrant.....	8
Figure 2 Baffled Mixing System.....	10
Figure 3 Interface Separation for $Zr(OH)_4$ sludge in 3 M NaOH at 1 and 3 wt%.....	12
Figure 4 Zirconium Hydroxide and Gibbsite Settled Solids Results .....	13
Figure 5 Impact of Aluminum Content of Settled Solids for Real and Simulated Tank Waste Sludge Samples.....	13
Figure 6 Normalized Settling Data vs $\phi/\phi_{max}$ with Westesen et al. 2022 and Wells et al. 2011.....	14
Figure 7 Precipitated Fe-Rich Sludge with (left) and without (right) Gibbsite .....	14
Figure 8 Precipitated Zirconium Hydroxide Sludge with (left) and without (right) Gibbsite .....	15
Figure 9 Slurry Viscosity versus Shear Rate for Fe and Zr Hydroxide Sludges .....	15
Figure 10 $N_{js}$ values for Gibbsite (a), Boehmite (b), and Iron Oxide (c) for different <i>CBD</i> ratios.....	16
Figure 11 Cumulative Particle Size Distribution.....	17
Figure 12 $N_{js}$ values for Sieved Iron Oxide at different <i>CBD</i> ratios .....	17
Figure 13 $N_{js}$ values for 150 $\mu m$ and 60 $\mu m$ Iron Oxide Particles .....	18

## Tables

Table 1 Sludge Volumes in Waste Tanks in the SE Quadrant.....	8
Table 2 Zirconium Hydroxide and Gibbsite Slurry Compositions .....	9
Table 3 Zirconium Hydroxide and Gibbsite Settling Results .....	13

## 1.0 Introduction

The Hanford site currently houses 56 million gallons of hazardous and radioactive waste stored in underground tanks. Hanford's tanks contain a mixture of supernate, water-soluble saltcake, and water-insoluble sludge. The saltcake and supernate will be processed to remove cesium, and then immobilized as low-activity waste. The tank sludges, on the other hand, contain the bulk of the radionuclides and will be pretreated separately and disposed of as high-level waste (HLW).

Olson (2011) includes WTP acceptance criteria that describe physical and chemical characteristics of the waste that must be certified as acceptable before the waste is transferred from the tanks to WTP. At present, significant challenges exist relative to the preparation and delivery of feed directly from waste tanks to the treatment plant. Recent advances in glass formulation have limited the need for sludge leaching and washing prior to transferring to the WTP. Specifically, the quantity of aluminum that can be accommodated in HLW glass has more than doubled, significantly diminishing the benefits of sludge leaching to glass production. However, aluminum phases, in particular gibbsite, still pose a substantial challenge to the mixing and transport of slurries from HLW tanks.

Sludge waste in the SE area of the Hanford site is rich in gibbsite and pose challenges to slurry sampling and transport requirements to meet the vitrification facility waste acceptance criteria. These waste streams may test the slurry mixing capabilities to effectively re-suspend the waste after deposition or may be susceptible to depositing in pipelines thus restricting the ability to transfer to the WTP. Addressing these challenges will be key to the success of deploying a direct feed HLW approach for sludge processing.

The focus of this LDRD project is to understand undissolved solids mixing, solids suspension, fluid blending and settling performance of Hanford tank waste sludge to address challenges associated with the preparation in delivery of HLW sludge to the WTP. Additionally, methods have been developed that can be effectively deployed on actual waste samples.

## 2.0 Background and Metrics

The delivery of Hanford tank waste to the WTP is governed by specific waste acceptance criteria to certify the waste is in an acceptable composition before being delivered to the WTP. The critical velocity ( $V_{cr}$ ), shown in Equation (1), is a key parameter that must be accurately characterized to determine if the waste is acceptable for transfer.

$$V_M = 1.85 \sqrt{g d_s \left( \frac{\rho_s}{\rho_L} - 1 \right)} C_V^{0.1536} (1 - C_V)^{0.3564} \left( \frac{d_s}{D} \right)^{-0.378} \left[ \frac{D \rho_L \sqrt{g d_s \left( \frac{\rho_s}{\rho_L} - 1 \right)}}{\mu_C} \right]^{0.09} \chi^{0.30} \quad (1)$$

Critical velocity is defined as the fluid transport velocity at which solid particles begin to deposit on the bottom of a straight horizontal transfer line during slurry transport (Poloski et al. 2009). The critical velocity depends on the physical properties of the solid particles and carrier fluid as well as the geometry of the slurry transport system (Oroskar 1980). Critical velocity has not been directly measured for actual waste samples and instead require the settling and deposition of solid particles to be correlated with the fluid transfer velocity that resulted in that condition. Operationally, the settling of solid particles in transport piping at the critical velocity are undesirable during waste-transfer operations because they are precursors to pipeline plugging that is potentially irreversible. Therefore, the critical velocity of each tank waste feed campaign should be accurately identified to determine if the waste feed will challenge the designed fluid transfer velocity. Due to the scale of material and waste characterization needed to measure the symptoms of critical velocity as well as challenges using a critical velocity model to capture the complex slurries at the Hanford site, a consideration of the just-suspended impeller speed  $N_{js}$  can be used to correlate the behavior. The  $N_{js}$  metric has been used in numerous studies that have evaluated the mobilization of non-cohesive particles under various flow conditions as is given in Paul et al. (2004) and is described as

$$N_{js} = S_z v^{0.1} \left[ \frac{g(\rho_s - \rho_L)}{\rho_L} \right]^{0.45} X^{0.13} d^{0.2} D^{-0.85} \quad (2)$$

where  $S_z$  is a dimensionless number that is a function of impeller type,  $X$  is the mass ratio of solids to liquid, and  $D$  is the impeller diameter. There are similar dependencies for both the critical velocity and just-suspended impeller speed on dimensional parameters such as density of the solid ( $\rho_s$ ) to density of the liquid ( $\rho_L$ ) that conclude changes in particle size density distribution (PSDD) should warrant a similar response. PSDDs for Hanford waste have been constructed and described in Wells et al. (2007 and 2011), however, this has shown to be very challenging as less than 20% of the Hanford sludge inventory is currently characterized by PSDDs. For this LDRD work, simple sludge simulants with known PSDDs were measured for their  $N_{js}$  value in an effort to establish a method to infer PSDDs for actual Hanford waste.

### 3.0 Experimental Methods

The equipment and methods described in this section were used to obtain experimental results for the physical property behavior of blending disparate waste streams and the minimum agitation speed for complete solid suspension,  $N_{js}$ .

#### 3.1 Characteristics of SE Area Sludge

Of the 28 double-shell tanks at Hanford, 25 are in the 200 East Area of the site. Figure 1 shows the sources of sludge in the SE quadrant along with the sludge volumes that are in the waste tanks in the SE quadrant from the best basis inventory (Tank Waste Information Network System, 2021) shown in Table 1.

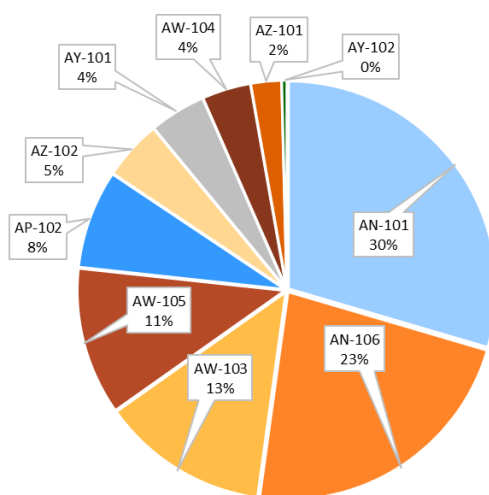


Figure 1 Sources of Sludge in the SE Quadrant

Table 1 Sludge Volumes in Waste Tanks in the SE Quadrant

Sludge Waste Type	Volume (kL)
NA	2140
Zr Cladding	2001
PUREX Cladding	1777
PUREX	1124
SRR	438
Bi-phosphate	411
FeCN	260
U Recovery	163
Thoria	149
Balance	142

The primary identified sludge layer is from the Zr cladding waste that is stored predominantly in tanks AW-103 and AW-105. The primary constituents of this waste are zirconium and uranium left from the fuel decladding. The next largest identified phase is from the PUREX cladding that was originally stored in the C-farms, but subsequently was transferred to tanks AN-101 and AN-

106. This stream consists predominantly of aluminum from the PUREX cladding in the mineral form of gibbsite. The NA sludge type is associated with waste phases for which the designation was lost as transfers were made, but the majority of the waste in this category originated as either PUREX cladding or Bi-phosphate waste. By volume, AN-101 and AN-106 contain most of the waste in the SE quadrant, followed by AW-103 and AW-105.

Recent simulant testing (Russell et al. 2009) using gibbsite and a precipitated hydroxide simulant indicated that blending materials with a drastically different physical properties can significantly alter the final slurry properties, potentially improving the slurry transport properties of wastes (such as those in the SE quadrant). As an important parameter to slurry transport, the settled solids measurements can help indicate slurry resuspension and transport challenges as it is reasonable to assume that slurries that settle to high solids loadings will be more difficult to suspend in a million gallon tank. This is partly due to the fact that at the same solids loading, these slurries will settle at significantly faster rates (Spearman and Manning, 2017). Thus, blending wastes that settle to high solids loadings with wastes that settle to low solids loadings should improve the slurry suspension and transport properties.

Characterization on waste from AW-105 and AN-106 indicated the Zr cladding material settled to a much lower solids loading (11 to 19%) in contrast to the PUREX cladding waste (29 to 67 wt%) (Sasaki, 1997). Based on the observed difference in physical parameters between the waste types, simulants were prepared to mimic these waste type behaviors and were blended to determine the resulting physical properties.

### 3.2 Settling Velocity

Hanford waste UDS particles are more dense than waste liquids are therefore will gravity-settle upon suspension in the liquid. A zirconium hydroxide simulant was prepared to represent AW-103 and AW-105 sludge waste by precipitating zirconium oxide with NaOH. Gibbsite ( $\text{Al}(\text{OH})_3$ ) was added to the Zr hydroxide sludge ( $\text{Zr}(\text{OH})_4$ ) in 3 M NaOH to prepare 8 different feed concentrations bounding initial solids concentrations between 1 and 20 wt%. Table 2 shows the specific components for each slurry feed.

Table 2 Zirconium Hydroxide and Gibbsite Slurry Compositions

Slurry ID	Zr(OH) <sub>4</sub> Sludge wt %	Al(OH) <sub>3</sub> wt %	Total wt%
Zr-A-1	1.4%	0.0%	1.4%
Zr-A-3	2.8%	0.0%	2.8%
Zr-B	0.4%	0.5%	0.9%
Zr-C	1.4%	4.0%	5.4%
Zr-D	1.9%	8.0%	10.0%
Zr-E	2.8%	16.2%	19.0%
Zr-F	8.5%	4.0%	12.5%
Zr-G	8.7%	1.4%	10.2%

Slurries were prepared in 125 mL bottles and shaken until homogenous. Samples were then transferred to a graduated cylinder and allowed to settle. The height of the sediment bed and total sample height were recorded as a function of time. As the samples settled, an interface developed between the turbid solution and clear supernate. The final sediment bed volume was measured after no significant change was observed in the height of this sludge layer over 1

hour. The volume percent settled solids were then determined by dividing the final sediment bed volume by the total volume of the slurry.

### 3.3 Shear Strength Measurements

Shear strength measurements of the Zr hydroxide sludge ( $\text{Zr}(\text{OH})_4$ ) sludge was determined with and without the presence of gibbsite ( $\text{Al}(\text{OH})_3$ ). Slurry rheology of the samples were measured using a Rotovisco RV20 Measuring System M equipped with an M5 measuring head (HAAKE Mess-Technik GmbH u. Co.) and an MV1 cup and rotor. Prior to the first measurement, the samples were mixed to uniformly suspend solids. Another measurement was taken after leaving the slurries undisturbed for 2 weeks. The test was performed by controlling the shear rate and measuring the shear stress. All tests were conducted at ambient temperature (22 °C).

### 3.4 Mixing Evaluation

The mixing tank used in this work was a cylindrical vessel fabricated to include stainless steel baffles. The material of the vessel was made of high-impact, SAN plastic to minimize any leaching or interaction with the caustic waste streams during mixing. The internal tank diameter,  $T$ , was 155 mm and its total height was 172 mm. A three-blade curved impeller was used as an agitator. Dimensions were measured with a caliper and were as follows: impeller diameter,  $D = 98.8$  mm; radius of curvature of the blades = 20.1 mm; height of the blade = 14.4 mm; and thickness of the blade = 1.4 mm. The impeller diameter-to-tank diameter ratio,  $D/T$ , was 0.63. The impeller was mounted on a shaft centrally located inside the mixing tank and was rotated by a Scilogex 20 L digital overhead stirrer. The tank was fully baffled made up of four stainless steel plates mounted from the top with the following dimensions: baffle width = 13.0 mm; baffle length = 147.6 mm. The baffle clearance was 16.7 mm from the vessel bottom and was placed 3.3 mm from the wall. A photograph of the mixing tank set up is shown in Figure 2.

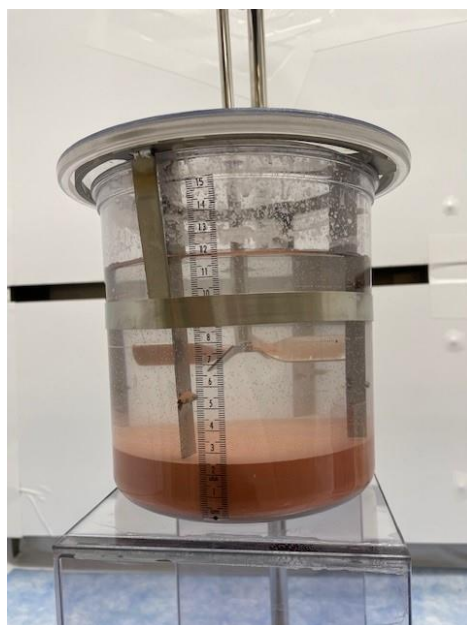


Figure 2 Baffled Mixing System

During a typical experiment, the mixing vessel was placed on an acrylic stand with cameras set up to the front and bottom so all necessary angles of the mixing tank could be clearly monitored. A dilute (0.1 M) NaOH solution at room temperature was always used as the liquid phase in the mixing tank. The slurries used in the solid suspension experiments were comprised individually of gibbsite ( $\text{Al}(\text{OH})_3$ ), boehmite ( $\text{AlOOH}$ ), iron oxide ( $\text{Fe}_2\text{O}_3$ ), and zirconium hydroxide ( $\text{Zr}(\text{OH})_4$ ). The solid mass to solution mass in the tank remained constant for all mixing experiments and was nominally 20 wt%.

A typical experimental run consisted of allowing the solids to settle in the tank for approximately 24 hours and then starting the agitation at low impeller speed and gradually increasing the speed in 25 rpm increments. The movement of the particles near the bottom of the tank as well as the flow pattern throughout the tank was carefully observed at each agitation speed. Solids suspension was observed visually via the camera set up below and front facing to the mixing tank, and the value of the agitation speed for complete off bottom suspension,  $N_{js}$ , was obtained and recorded. The criterion here to visually determine  $N_{js}$  was defined by Zwietering (1958), as the speed which no particles were visually observed to be at rest on the tank bottom for more than one or two seconds. This procedure was followed to obtain  $N_{js}$  in all experiments. This procedure was applied from repetitive experiments as well as spin down operations to determine when solids began to settle at the bottom of the tank to acquire consistent data. The digital cameras focused on the mixing vessel's front and bottom was also used to create a permanent record of the observations.  $N_{js}$  was experimentally obtained for different values of the following operation variables:

- Impeller off-bottom clearance (40, 50, and 60 mm)
- Solids particle size
- Identical experiments are different times to determine experimental reproducibility. The reproducibility experiments were typically found to be  $\pm 5\%$ .

## 4.0 Results

Simulant slurry experiments were conducted to determine the physical property behavior in terms of undissolved solids mixing, solids suspension, fluid blending and settling performance. Below are the results from the executed tests.

### 4.1 Impact of Al Content on Settle Solids

The eight matrices described in Table 2 were settled to assess the impact of increasing Al concentration on settling rate and final settled solids concentration. The behavior of interface separation across different solids loadings for the  $\text{Zr}(\text{OH})_4$  sludge without the presence of added Al is shown in Figure 3.

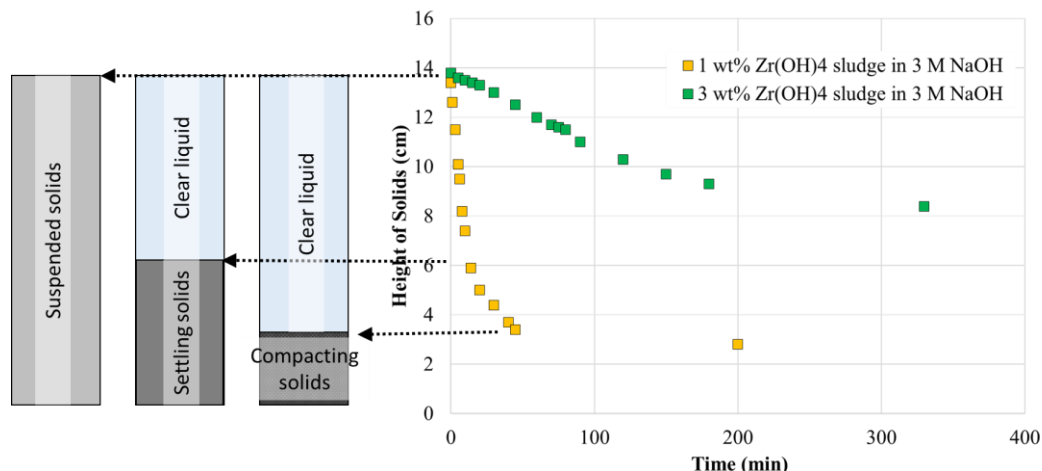


Figure 3 Interface Separation for  $Zr(OH)_4$  sludge in 3 M NaOH at 1 and 3 wt%

Both of the level-versus-time profiles for the  $Zr(OH)_4$  sludge (without added gibbsite) exhibited a linear decrease in level (constant interface velocity during settling), followed by a period of smaller change in level as compaction proceeded. The “fast” interface velocities of the initial settling periods of the tests were calculated as  $6.1E-1$  cm/min for the 1-wt% sludge and  $2.9E-2$  cm/min for the 3-wt% sludge. The fact that the interface velocities in these two tests with equivalent particulate had two distinct values is assumed to be due solely to the different solids concentrations (i.e., hindered settling effects only).

A summary of the final compacted sediment with mass fraction of gibbsite is tabulated in Table 3 with a graph of the data displayed in Figure 4. As can be seen from the data, there is a reasonable trend between increasing mass fraction of gibbsite and increased settled solids concentration. This data was compared to previous settling tests by Westesen et al. 2023 that determined the change in physical properties of an iron rich sludge containing  $FeOOH$  with various concentrations of gibbsite as well as as-found Hanford tank samples from AN-106 in Figure 5. In all cases, increasing wt% Al in the slurries resulted in an increase in the final settled solids concentration, suggesting that gibbsite particles will pack to a very dense layer prior to slurry mobilization. An overall deviation of nominally 30% in the settled solids wt% is seen between the AN-106 waste samples and the tested Zr and Fe simulants. After gibbsite, the largest insoluble components in the AN-106 waste are natrophosphate and clarkeite. These constituents have large particles that dominate the settling properties when the mass fraction of gibbsite is low and settle to nominally 25 wt%. Note that an increase in settled solids loading directly leads to faster settling rates (Williams et al. 2023). Thus, adjusting the gibbsite mass fraction appears to directly affect the physical properties of the slurry and in particular the settling rate. In regard to WTP operations, slurries that settle too fast and cannot be effectively sampled or transferred, appear to be remediated by blending with waste streams of disparate behaviors.

Table 3 Zirconium Hydroxide and Gibbsite Settling Results

Slurry ID	Wt% Solids in Final Compacted Sediment	Mass fraction Gibbsite, %
Zr-A-1	6%	0%
Zr-A-3	5%	0%
Zr-B	16%	58%
Zr-C	20%	74%
Zr-D	27%	81%
Zr-E	38%	85%
Zr-F	14%	32%
Zr-G	9%	14%

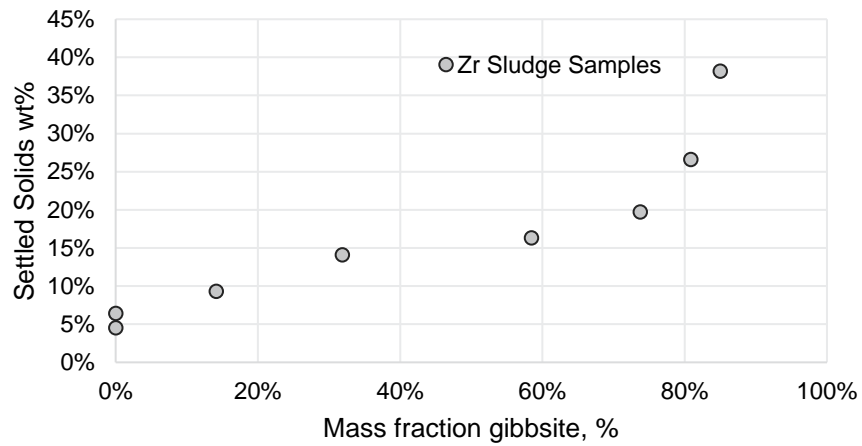


Figure 4 Zirconium Hydroxide and Gibbsite Settled Solids Results

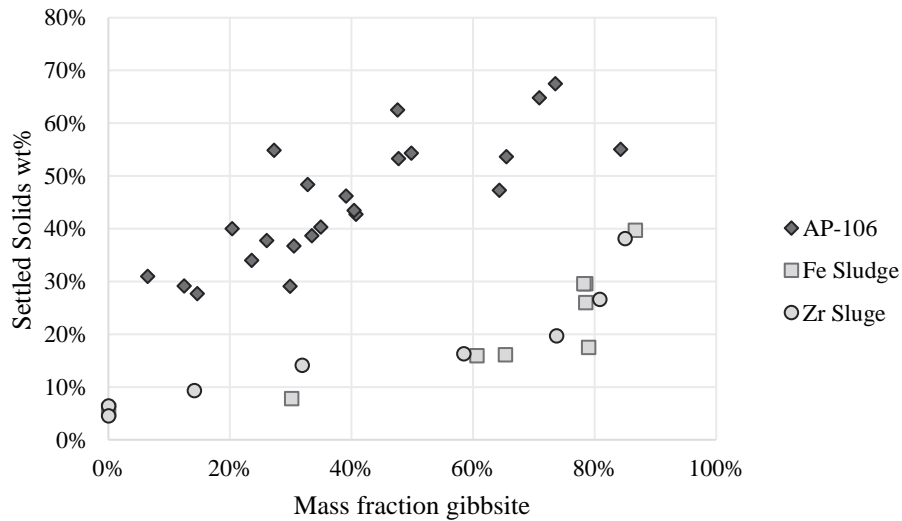


Figure 5 Impact of Aluminum Content of Settled Solids for Real and Simulated Tank Waste Sludge Samples.

The hindered settling rate data normalized to the initial settling rate ( $w/w_0$ ) and the initial volume ratio normalized to the maximum solids loading ( $\Phi/\Phi_{max}$ ) is shown in Figure 6. Normalizing the data in this way allows for a direct comparison of settling rates along a wide array of behaviors. Data obtained from the work reported herein was compared against previous LDRD data with simulants (Westesen et al. 2022) and settling studies conducted on a variety of Hanford tank sludge (Wells et al. 2011). Data points near a  $\Phi/\Phi_{max}$  of 1 are difficult to measure and deviate from the fit, however, despite a large distribution of  $\Phi_{max}$  values, all samples tested appear to align with this general fit.

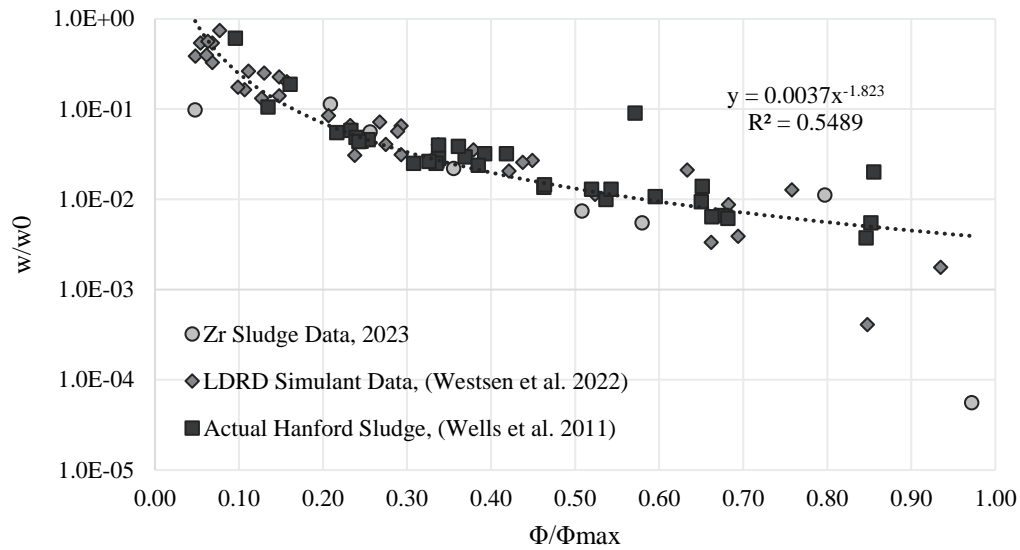
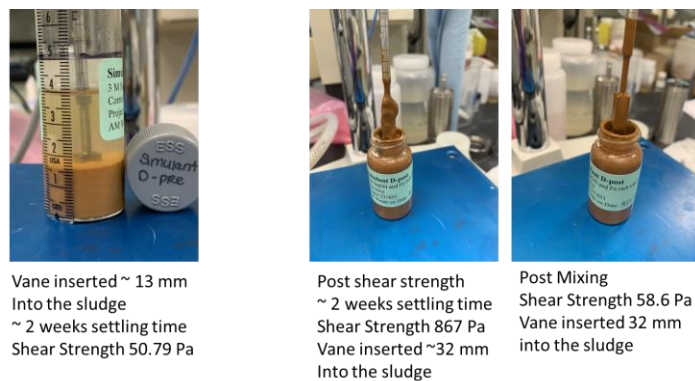


Figure 6 Normalized Settling Data vs  $\phi/\phi_{max}$  with Westesen et al. 2022 and Wells et al. 2011

## 4.2 Rheology of Samples

An evaluation of the shear stress for the precipitated Fe-rich sludge the zirconium hydroxide sludge was determined with and without the presence of gibbsite. Since gibbsite settles to a high solids loading, it's thought the shear strength of the bed is increased with increasing amounts of gibbsite. Figure 7 and Figure 8 show visually what the shear vane measurements looked like. For this testing “pre” is designated as samples with gibbsite, and “post” are samples without gibbsite.



Vane inserted ~ 13 mm into the sludge  
~ 2 weeks settling time  
Shear Strength 50.79 Pa

Post shear strength  
~ 2 weeks settling time  
Shear Strength 867 Pa  
Vane inserted ~32 mm into the sludge

Post Mixing  
Shear Strength 58.6 Pa  
Vane inserted 32 mm into the sludge

Figure 7 Precipitated Fe-Rich Sludge with (left) and without (right) Gibbsite

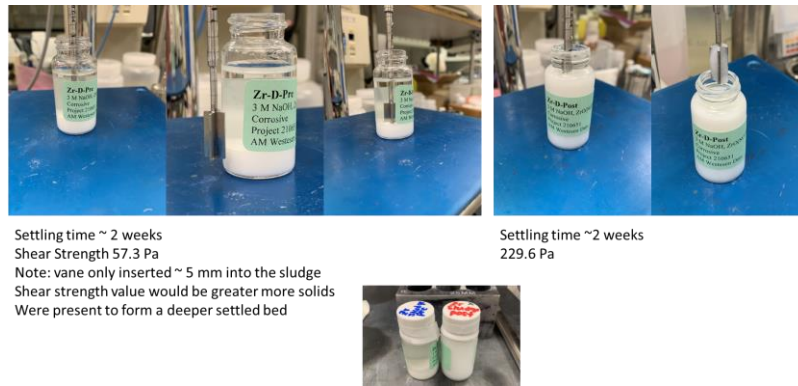
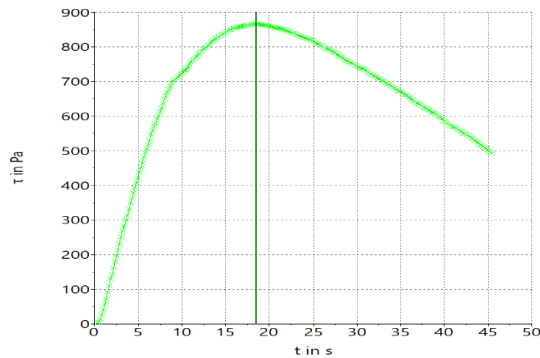


Figure 8 Precipitated Zirconium Hydroxide Sludge with (left) and without (right) Gibbsite

In both cases, samples with gibbsite had a lower shear strength. This is thought to be attributed to the granular nature of the gibbsite decreasing the rheology of the sticky sludges when combined. Both sludges interacted similarly in the absence of gibbsite causing the settled solids shear strength to increase. Figure 9 presents shear stress-shear rate-viscosity curves characteristic of this data set. The last point highlighted in the figure presents the measured shear stress as a function of the controlled shear rate. A two-week settling time was conducted on the sludge samples without gibbsite and showed shear strength measurements of 867 Pa for the Fe-hydroxide sludge and 230 Pa for the Zr-hydroxide sludge.

a) Precipitated Fe-Hydroxide Sludge



b) Zirconium-Hydroxide Sludge

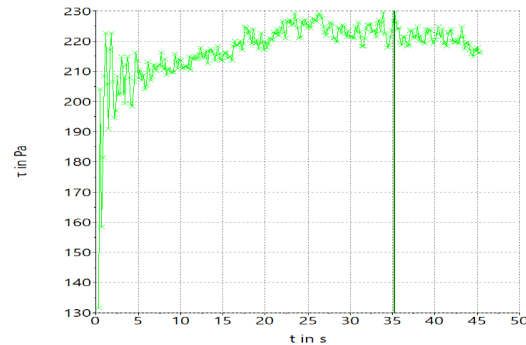


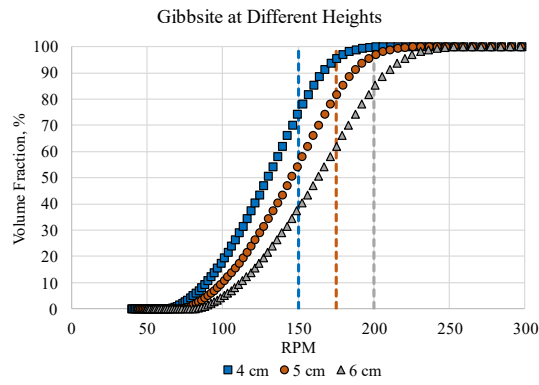
Figure 9 Slurry Viscosity versus Shear Rate for Fe and Zr Hydroxide Sludges

### 4.3 Solid Suspension Mixing Experiments

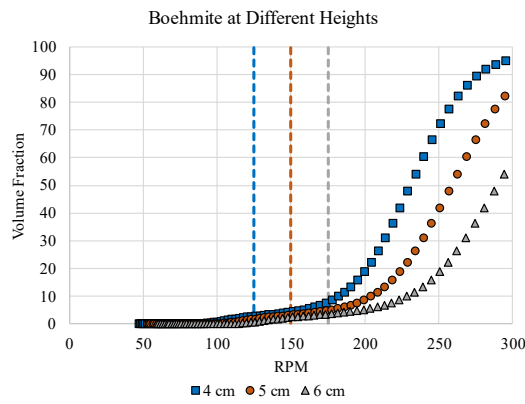
The values of  $N_{js}$  were experimentally obtained for different  $C_B/D$  ratios for the solid suspension system. The results obtained using gibbsite, boehmite, and red iron oxide are shown in Figure 10. There is excellent consistency between the volume fraction and RPM value needed to suspend the solids for each slurry tested. The  $N_{js}$  values increase proportionately with the increase in blade height above the bottom of the mixing vessel. As to be expected, solid suspension was more easily achieved at a low impeller clearance. The data presented for the lowest impeller clearance value (4 cm above vessel bottom) corresponded to  $C_B/D$  value of 0.26 while the highest clearance value (6 cm above vessel bottom) corresponded to a  $C_B/D$  value of 0.39. Solid suspension with larger particles (red iron oxide) resulted in larger  $N_{js}$  values than smaller particle suspension (gibbsite). However, the lowest value of  $N_{js}$  for this system (125 RPM) was obtained for boehmite at a  $C_B/D = 0.26$ . Particle size distribution (PSD) measurements of each of the constituents (shown in Figure 11) indicate gibbsite should have a

lower experimental  $N_{js}$  value compared to boehmite. It's possible the dense layer formed by the settled gibbsite particles resulted in an increase RPM required to suspend the solids.

a)



b)



c)

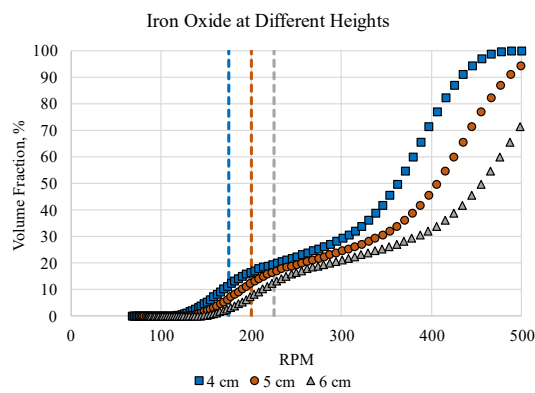


Figure 10  $N_{js}$  values for Gibbsite (a), Boehmite (b), and Iron Oxide (c) for different  $C_B/D$  ratios

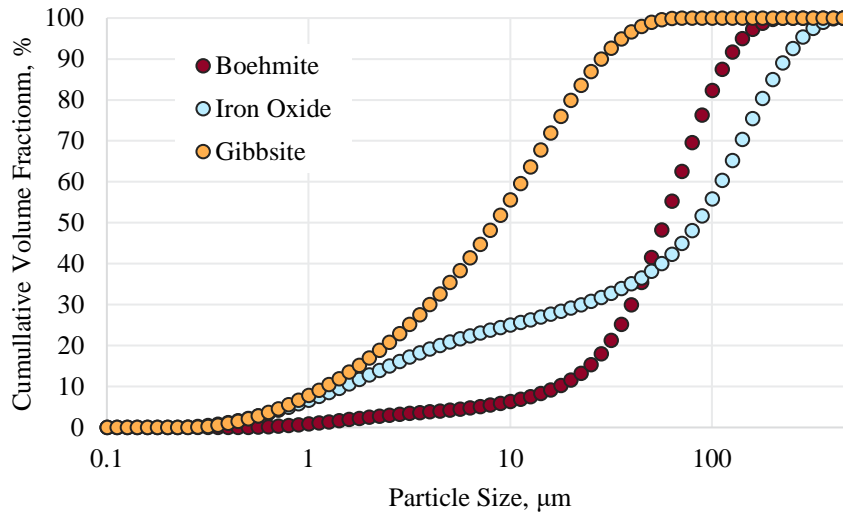


Figure 11 Cumulative Particle Size Distribution

The iron oxide was sieved to compare experiments with the as-received 150 μm particles to 60 μm particles. The results for the sieved iron oxide data obtained at 2 cm, 3 cm, and 4 cm are shown in Figure 12. The data showed that the  $N_{js}$  varied consistency with the  $C_B/D$  despite the difference in particle size from the as-received. Interestingly, when comparing the experimental data between the two sieve sizes at 4 cm, similar to the gibbsite and boehmite experimental data, the larger iron oxide particles produced the smaller  $N_{js}$  values (shown in Figure 13) and may also be attributed to densely packed bed before mixing.

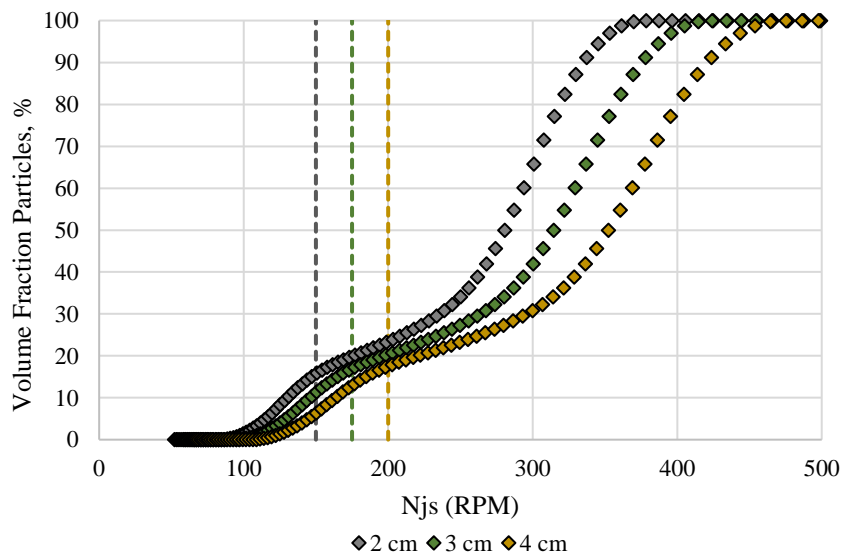


Figure 12  $N_{js}$  values for Sieved Iron Oxide at different  $C_B/D$  ratios

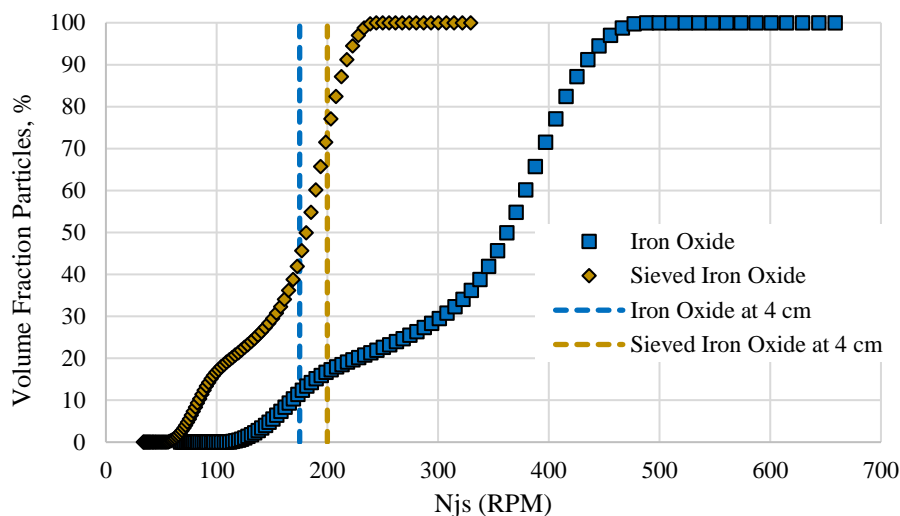


Figure 13  $N_{js}$  values for 150  $\mu\text{m}$  and 60  $\mu\text{m}$  Iron Oxide Particles

Due to the difficulty in measuring PSD values on actual waste samples, having a capability to experimentally determine  $N_{js}$  values with simple simulants and known PSD's can be used to compare like behaviors with actual waste sludge as a method to experimentally derive PSD values. Additional simulants representing phases in actual waste sludge can continue to support filling in the gaps around actual waste behavior to help inform operational flowsheet development underway for HLW.

## 5.0 Conclusions

An assessment of slurry settling, shear strength, and just suspended impeller speed ( $N_{js}$ ) was conducted on various simple simulants to help understand predictive capabilities of HLW solids settling and transport as well as help provide technical guidance during HLW flowsheet planning.

Existing high-level waste sludge data has shown the effect that increasing Al concentration has on resulting settled solids. This differential settling of particles in the sludge has the possibility of resulting in solids segregation during feed preparation and uneven particle distribution during pipeline transportation or mixer jet pump operations. Settling studies conducted on a zirconium hydroxide sludge with various amounts of gibbsite added determined increasing wt% Al in the slurries resulted in an increase in the final settled solids concentration, suggesting that gibbsite particles will pack to a very dense layer prior to slurry mobilization. Normalized hindered settling rate to settled solids concentration showed good agreement in behavior between LDRD simulant data and a wide variety of Hanford tank sludge. Adjusting the gibbsite mass fraction appeared to directly affect the physical properties of the slurry and in particular the settling rate. In regard to WTP operations, slurries that settle too fast and cannot be effectively sampled or transferred, may be remediated by blending with waste streams of disparate behaviors.

Shear strength measurements of Fe and Zr hydroxide slurries with and without gibbsite showed samples with gibbsite had a lower shear strength than samples without. Although contrary to the prediction based on settled solids wt% in the bed, this is thought to be attributed to the granular nature of the gibbsite decreasing the rheology of the sticky slurries when combined.

Experimental  $N_{js}$  values were obtained in a mixing system at different  $C_B/D$  ratios. In all cases, there was excellent consistency between the volume fraction and RPM value needed to suspend the solids. Additionally, the  $N_{js}$  values increased proportionately with the increases in blade height above the bottom of the mixing vessel. Discrepancies between experimentally determined  $N_{js}$  values and predicted  $N_{js}$  values were seen between gibbsite and boehmite, where the larger boehmite particles consistently resulted in a lower  $N_{js}$  value than the smaller gibbsite particles. This may be due to the densely packed bed that gibbsite forms when settled in the bottom of the mixing vessel. Data collected with simple simulants and known PSDDs can be used as a method to experimentally determine PSDD measurements for actual waste sludge. Additional simulants representing phases in actual waste sludge can continue to support filling in the gaps around actual waste behavior to help inform operational flowsheet development underway for HLW.

## 6.0 References

Olson JW. 2011. ICD 19 - Interface Control Document for Waste Feed. 24590-WTP-ICD-MG-01-019, Rev 5. River Protection Project, Waste Treatment Plant, Richland, WA.

Oroskar AR and RM Turian. 1980. "The critical velocity in pipeline flow of slurries." *AIChE Journal* 26 (4) pp. 550-558.

Paul EL, VA Atiemo-Obeng, and SM Kresta. 2004. *Handbook of Industrial Mixing Science and Practice*. John Wiley & Sons, Inc., Hoboken, New Jersey.

Poloski, Adam P., Adkins, Harold E., Abrefah, John, Casella, Andrew M., Hohimer, Ryan E., Nigl, Franz, Minette, Michael J., Toth, James J., Tingey, Joel M., and Yokuda, Satoru T. *Deposition Velocities of Newtonian and Non-Newtonian Slurries in Pipelines*. United States: N. p., 2009. Web. doi:10.2172/963206.

Russell RL, et al. 2009. "Validation of Ultrafilter Performance Model Based on Systematic Simulant Evaluation." *Industrial & Engineering Chemistry Research* 48(22):10077-10086.

Sasaki LM. 1997. Tank Characterization Report for Double-Shell Tank 241-AW-105. HNF-SD-WM-ER-364 Rev. 1. Lockheed Martin Hanford Corporation, Richland, WA. p. 232.

Spearman J and AJ Manning. 2017. "On the hindered settling of sand-mud suspensions." *Ocean Dynamics* 67(3-4):465-483.

Tank Waste Information Network System. 2021. Available from: [https://twins.hanford.gov/Forms/BuildQuery.aspx?SourceName=bb\\_published.dbo.p\\_calc\\_detail&whatsnew=Best|Basis|Inventory](https://twins.hanford.gov/Forms/BuildQuery.aspx?SourceName=bb_published.dbo.p_calc_detail&whatsnew=Best|Basis|Inventory).

Wells BE, MA Knight, EC Buck, SK Cooley, RC Daniel, LA Mahoney, PA Meyer, AP Poloski, JM Tingey, WS Callaway III, GA Cooke, ME Johnson, MG Thien, DJ Washenfelder, JJ Davis, MN Hall, GL Smith, SL Thomson, and Y Onishi. 2007. Estimate of Hanford Waste Insoluble Solid Particle Size and Density Distribution. PNWD-3824 (WTP-RPT-153, Rev. 0), Battelle—Pacific Northwest Division, Richland, Washington.

Wells BE, DE Kurath, LA Mahoney, Y Onishi, JL Huckaby, SK Cooley, CA Burns, EC Buck, JM Tingey, RC Daniel, and KK Anderson. 2011. Hanford Waste Physical and Rheological Properties: Data and Gaps. PNNL-20646. Pacific Northwest National Laboratory, Richland Washington.

Westesen AM, AN Williams, RA Peterson, and CA Burns. 2022. Sludge Processing Options for early HLW Treatment at Hanford. PNNL-33355. Pacific Northwest National Laboratory, Richland Washington.

Westesen AM, AM Robb, NL Cappella, C Alvarez, RA Peterson. 2023. Phosphate and Fluoride Processing Options for Hanford Sludge. PNNL-34456. Pacific Northwest National Laboratory, Richland Washington.

Williams AN, AM Westesen, and RA Peterson. 2023. "The evaluation of aluminum and iron metal oxide settling behaviors for Hanford insoluble solids waste preprocessing." *Environmental Progress & Sustainable Energy*.

Zwietering, T. N., Suspending of solid particles in liquid by agitators. *Chemical Engineering Science*, 1958, 8:244.

# **Pacific Northwest National Laboratory**

902 Battelle Boulevard  
P.O. Box 999  
Richland, WA 99354

1-888-375-PNNL (7665)

***[www.pnnl.gov](http://www.pnnl.gov)***